Theoretical Studies on the Excited States, DNA Photocleavage, and Spectral Properties of Complex $[Ru(phen)_2(6\text{-OH-dppz})]^{2+}$

Lian-Cai Xu, Jun Li, Yong Shen, Kang-Cheng Zheng,* and Liang-Nian Ji*

School of Chemistry and Chemical Engineering, The Key Laboratory of Gene Engineering of Ministry of Education, State Key Laboratory of Optoelectronic Materials and Technologies, Zhongshan (Sun Yat-Sen) University, Guangzhou 510275, People's Republic of China

Received: July 4, 2006; In Final Form: October 23, 2006

The structures and related properties of the complex $[Ru(phen)_2(6\text{-OH-dppz})]^{2+}$ (phen = 1,10-phenanthroline; dppz = dipyrido [3,2-*a*:2′,3′-*c*]phenazine) in the ground state (S_0), the first singlet excited state (S_1), and the first triplet excited state (T_1) have been studied using density functional theory (DFT), time-dependent (TD) DFT, Hartree−Fock (HF), and configuration interaction singles (CIS) methods. Three electronic absorption-spectral bands (^{1}MLCT, ^{1}LL, and ^{1}LL) lying in the range of 250−550 nm in vacuo and in aqueous solution were theoretically calculated, simulated, and assigned with TDDFT method. In particular, the theoretical results show the following: (1) The positive charges of central Ru atom in the excited states (S_1 and T_1) are greatly increased relative to those in the ground state (S_0), and thus the Ru atom in the excited states can be regarded as Ru(III). (2) The positive charges on the main ligand (6-OH-dppz) in the excited states are considerably reduced, and thus the interaction between the main ligand (intercalative ligand) and DNA base pairs is considerably weakened. (3) The geometric structures in excited states are also distorted, resulting in obvious increase in the coordination bond length. It is advantageous to the complex forming a high oxidizing center (i.e., Ru(III) ion). On the basis of these results, a theoretical explanation on photoinduced oxidation reduction mechanism of DNA photocleavage by $[Ru(phen)_2(6\text{-OH-dppz})]^{2+}$ has been presented.

1. Introduction

During the past decade, the transition-metal complexes containing bipyridine (bpy) and phenanthroline (phen) or their modified moieties as ligands have attracted considerable interest for their potential utilities in DNA-cleavage agents,[1,2] DNA structure probes,[3,4] DNA photoprobes,[5] DNA molecular light switches,[6,7] and so forth. Recently, many transition-metal polypyridyl complexes have been synthesized and characterized, and their DNA-binding properties have been investigated by UV−vis absorption spectra, emission spectra, viscosity measurement, circular dichroism spectra and gel electrophoresis experiments, and so forth.[7−10] Moreover, some of them have been found to possess an excellent DNA cleavage characteristic under light irradiation,[7−10] in agreement with the statement "those complexes whose excited states can initiate a series of chemical reactions which ultimately lead to nucleic acid cleavage" in the review.[11]

At present, many interests have been focused on DNA photocleavage by Ru(II) polypyridyl-type complexes, because such a kind of complex can bind to DNA in an intercalative mode which is the most important and well-known mode in the interactions between the complex and DNA. The clarification of the DNA-photocleavage mechanism of such complexes will be very helpful to the comprehension of the trend in DNA mutation and damage as well as further to the design of DNA photocleavage agents. On the basis of a great number of experimental studies, two main DNA-photocleavage mechanisms by Ru(II) complexes, that is, the $^1O_2$ mechanism[11,12−13] and the photoelectron transfer[11,14−17] (or called photoinduced oxidation reduction) mechanism, have been presented. However, it is still difficult to tell out the DNA photocleavage belonging to which kind of special mechanism for a given Ru(II) complex.[18−19]As is well known, the photoinduced DNA cleavage by the Ru(II) polypyridyl complexes closely relates to the electronic properties of excited states, moreover, as far as we have known, the theoretical report based on the electronic excited states of transition metal complexes to explain the DNA photocleavage mechanism has not been found yet. It may be such a reason that a great deal of computational expense is required for the study on the excited states of transition metal complexes. Along with the high-speed development of computer technology, the studies on the electronic structures and related properties of the excited states of transition-metal complexes have become a conspicuous theoretical project.[20−25]

On the other hand, it is very important to investigate the spectral properties of complexes due to their close relating to the photochemistry and photophysics of complexes. Recently, more and more theoretical computations applying the time-dependent density functional theory (TDDFT) method[26−32] have been reported. The TDDFT method has successfully been used to calculate the electronic spectra of medium-sized and large molecules (up to 200 second-row atoms)[33,34] and also has been used to calculate the electronic spectra of some transition metal complexes including Ru(II) complexes,[20−24,35,36] although TD-DFT still introduces errors by using the approximate exchange-correlation (xc) functional, and is being improved for long-range charge-transfer excited states.[37,38] However, the TDDFT studies on the spectral properties of such a kind of complex in vacuo and in aqueous solution are still preliminary.[20,23,25,35]

The complexes $[Ru(L)_2(dppz)]^{2+}$ (L = phen, bpy) are not only well-known DNA "light switch" complexes but also

* To whom correspondence should be addressed. E-mail: ceszkc@zsu.edu.cn (K.-C.Z.); cesjln@zsu.edu.cn (L.-N.J.).

10.1021/jp064189y CCC: $37.00
Published on Web 12/19/2006

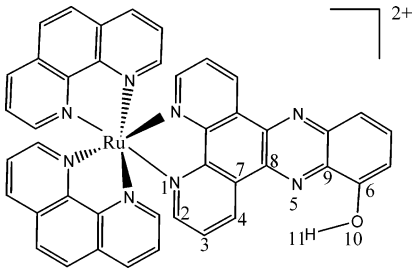

Figure 1. Structural schematic diagram of $[Ru(phen)_2(6\text{-OH-dppz})]^{2+}$ and atomic labels.

potential DNA-photocleavage agents.[17,39] Barton et al.[17] first reported that the photoexcited $[Ru(phen)_2(dppz)]^{2+}$ intercalator in DNA quenched by electron acceptor can generate Ru(III) resulting in the damage of DNA. Recently, Yavin et al.[39] also found that the $[Ru(phen)_2(dppz)]^{2+}$ can cause the single-strand cleavage of DNA through irradiation. In addition, the experimental[40] and theoretical studies[23,41] on complexes $[Ru(L)_2(dppz)]^{2+}$ (L = phen, bpy) have shown that their "light switch" behaviors closely correlate to the presence of the low lying excited states. However, so far the theoretical studies on the properties of low lying excited states of these Ru(II) complexes, especially ones containing substitutive groups on dppz, are rather rare. More recently, some complexes have been synthesized by introducing substituent into dppz and characterized.[7] Moreover, it is interesting to find that $[Ru(phen)_2(6\text{-OH-dppz})]^{2+}$ can well cause the cleavage of a single strand of DNA under irradiation and show considerable "light switch" behavior in which the complex emits weak luminescence in aqueous solution at the absence of DNA and strong luminescence at the presence of DNA. Obviously, the complex $[Ru(phen)_2(6\text{-OH-dppz})]^{2+}$ and its parent $[Ru(phen)_2(dppz)]^{2+}$ have many common characteristics in photochemical properties. Therefore, it is very significant to study the properties of the excited states of $[Ru(phen)_2(6\text{-OH-dppz})]^{2+}$ as an example for exploring the DNA-photocleavage mechanism by this kind of Ru(II) complex as well as the effect of subsitituent OH on the related properties.

In this paper, we report on the structures and related properties of the complex $[Ru(phen)_2(6\text{-OH-dppz})]^{2+}$ in the ground state (S_0), the first singlet excited state (S_1), and the first triplet excited state (T_1) using DFT, TDDFT, Hartree−Fock (HF), and configuration interaction singles (CIS) methods. This article mainly reveals the characteristics of geometric and electronic structures of the complex in the excited states, which are much different from those in the ground state, and hereby presents a new insight on the explanation of DNA photocleavage at the level of electronic structure. In addition, the electronic absorption spectra of the complex are also computed, assigned and simulated with the DFT/TDDFT methods.

2. Computational Methods

Structural schematic diagram of the studied complex is shown in Figure 1. The complex $[Ru(phen)_2(6\text{-OH-dppz})]^{2+}$ forms from a Ru(II) ion, one main ligand (or called as intercalative ligand) (6-OH-dppz), and two co-ligands (phen), and has no symmetry. The geometry optimization of the complex in the ground state (S_0) was carried out using the DFT, HF, and second-order Møller-Plesset perturbation (MP2)[42−44] (for comparison) methods, respectively. For the obtained structures with the methods of DFT-B3LYP and HF, the frequency calculations were also performed to verify the optimized structure to be at an energy minimum. The geometries of the lowest singlet excited state (S_1) and triplet excited state (T_1) of the complex were fully optimized using the CIS method,[45] and for an effective comparison, the ground structure at the level of HF was used as the preliminary structure for the excited-state optimization. The natural population analyses (NPA) were further carried out for the ground state with HF method and for the excited states with CIS method on the basis of their corresponding optimized geometries. The electronic absorption spectra in vacuo and in aqueous solution were calculated with the TDDFT method at the B3LYP/LanL2DZ level, and 90 singlet-excited-state energies of the complex were calculated. The conductor polarizable continuum model (CPCM)[46,47] was applied to the solvent effect in aqueous solution. LanL2DZ basis set[48,49] was adopted for all the calculations with Gaussian03 program-package (revision D.01).[50] In addition, in order to easily and clearly understand the related properties of the complex, the schematic diagrams of some related frontier molecular orbitals of the complex for the S_0 state were drawn with the Molden v3.7 program[51] based on the DFT computational results.

3. Results and Discussion

3.1. The Ground-State (S_0) and Lowest Excited-State (S_1, T_1) Geometries. The calculated geometrical parameters of S_0, S_1, and T_1 states of $[Ru(phen)_2(6\text{-OH-dppz})]^{2+}$ were selectively listed in Table 1 (atomic labels shown in Figure 1). For comparison, the corresponding X-ray data of the analogs $[Ru(dmp)_2(dppz)](PF_6)_2$[52] were also given in Table 1.

So far, the experimental crystal structure of complex $[Ru(phen)_2(6\text{-OH-dppz})]^{2+}$ has not been found yet; we cannot directly compare the calculated geometric structure with experimental one. However, we can compare the optimized geometric structure of $[Ru(phen)_2(6\text{-OH-dppz})]^{2+}$ with the structure of the analogs $[Ru(dmp)_2(dppz)](PF_6)_2$ (dmp = 2,9-dimethyl-1,10-phenanthroline), which has the X-ray data.[52] The computational results in the ground state for $[Ru(phen)_2(6\text{-OH-dppz})]^{2+}$ are reliable because they quite near the reported experimental values of the analogs $[Ru(dmp)_2(dppz)](PF_6)_2$[52] (seen in Table 1) of which the mean coordination bond length between center Ru atom and N atoms of main ligand is 0.2096 nm and that between center Ru atom and N atoms of coligands is 0.2108 nm. It is easy to see that the geometric parameters optimized by the DFT method are more consistent with the corresponding experimental data than those by the MP2 and HF methods, respectively.

The deviation of the geometric parameters optimized by the HF method from the corresponding experimental data of $[Ru(dmp)_2(dppz)](PF_6)_2]$ is ∼4% for mean coordination bond length and ∼2% for mean coordination bond angle. Therefore, the optimized geometric structure of the complex in the ground state with the HF method is still substantially receivable. Though, in order to reasonably perform the comparisons of the structures and charge properties for the ground state with those for the excited states, the HF results were adopted for the ground state, and the CIS results were adopted for the excited states because the CIS method belongs to post HF method.

From Table 1, we can see that the changes of coordination bond lengths and bond angles of the complex in the excited states (S_1, T_1) relative to the ground state are considerable. First, for the first singlet state (S_1), the mean bond length of the main ligand ($Ru-N_m$) is increased by 0.0069 nm and that of the coligand ($Ru-N_{co}$) is also increased by 0.0150 nm; the coordination bond angle between the central Ru atom and the N atoms of the main ligand is reduced by 1.96° and that of the coligand is reduced by 4.57°. Second, for the first triplet state (T_1), the changes in the bond lengths and the bond angles

TABLE 1: Selected Bond Lengths in Nanometer and Bond Angles in Degree for the Ground State (S_0) with HF, MP2, and B3LYP Methods, Respectively, as well as Those for the Lowest Singlet Excited State (S_1) and the Lowest Triplet Excited State (T_1) of $[Ru\ (phen)_2(6\text{-OH-dppz})]^{2+}$ with the CIS Method

state[a]	Ru−N_m[b]	Ru−N_{co}[b]	C−$C(N)_m$[c]	C−$C(N)_{co}$[c]	C_6−O_{10}/O_{10}−H_{11}	N_5−H_{11}	θ_m[d]	θ_{co}[d]	β[d]
S_0^{B3LYP}	0.2106	0.2107	0.1405	0.1405	0.1375/0.0983	0.2283	79.16	79.44	0.00
S_0^{MP2}	0.2075	0.2078	0.1423	0.1423	0.1402/0.0989	0.2324	80.35	80.50	−0.07
S_0^{HF}	0.2181	0.2184	0.1389	0.1391	0.1365/0.0953	0.2367	77.17	77.55	0.13
(expt)[e]	0.2096	0.2108					78.86	79.13	
$S_1^{CIS//HF}$	0.2250	0.2334	0.1390	0.1391	0.1365/0.0953	0.2367	75.21	72.83	0.17
$T_1^{CIS//HF}$	0.2320	0.2311	0.1390	0.1391	0.1365/0.0953	0.2366	73.00	73.49	0.09

[a] Superscript means the calculation method. [b] Ru−N_m is the average coordination bond length between the central atom and the main ligand (OH-dppz), and Ru−N_{co} is that between the central atom and the coligand (phen). [c] C−$C(N)_m$ is the mean bond length of the skeleton of the main ligand, and C−$C(N)_{co}$ is that of the coligands (phen). [d] θ_m is the coordination bond angle of the central atom and the two N atoms of the main ligand, and θ_{co} is that of the central atom and the two N atoms of coligand (phen), β is the dihedral angle C_9−C_6−O_{10}−H_{11}. [e] The X-ray data of the analogs $[Ru(dmp)_2(dppz)](PF_6)_2$.[52]

TABLE 2: Related Natural Charge Populations (|e|) of $[Ru(phen)_2(6\text{-OH-dppz})]^{2+}$ in the Ground State (S_0) at HF/LanL2DZ Level, and in the First Singlet Excited State (S_1), and the First Triplet Excited State (T_1) at CIS/LanL2DZ Level

state	Ru	N_1	C_2	C_3	C_4	N_5	C_6
S_0^{HF}	0.9809	−0.5854	0.1592	−0.2344	−0.0787	−0.5008	0.4047
$S_1^{CIS//HF}$	1.1772	−0.6071	0.1607	−0.2367	−0.0769	−0.5009	0.4048
$T_1^{CIS//HF}$	1.1850	−0.6123	0.1559	−0.2357	−0.0804	−0.5010	0.4047

	C_7	C_8	C_9	OH	main-L	co-L
S_0^{HF}	−0.0757	0.2081	0.1267	−0.2508	0.3397	0.6794
$S_1^{CIS//HF}$	−0.0780	0.2082	0.1270	−0.2507	0.2939	0.5289
$T_1^{CIS//HF}$	−0.0757	0.2081	0.1270	−0.2508	0.2693	0.5457

(relative to S_0) are also obvious. The mean coordination bond length between the metal ion and the N atoms of the main ligand is increased by 0.0139 nm, and that of the coligand is increased by 0.0127 nm. The bond angle between the central Ru atom and the N atoms of the main ligand is reduced by 4.17° and that of the coligand is reduced by 4.06°. In addition, all the dihedral angles in the main ligand are near 0.0°, and such a result shows the planarity of the main ligand for all these different states is excellent.

3.2. Natural Charge Populations of the Complex in the S_0, S_1, and T_1 States. The natural charge populations of the complex in the S_0, S_1, and T_1 states from the natural orbital population analysis (NPA) on the basis of their corresponding optimized geometric structures (the atomic labels displayed in Figure 1) are listed in Table 2.

In general, the natural charge populations of a complex closely relate to its chemical properties. It is very interesting to find that the natural charge populations of the complex in the S_1 and T_1 states are very different from those in the S_0 state. The positive net charges of the Ru atom greatly increase from 0.9809 (|e|) in the S_0 state to 1.1772 (|e|) in the S_1 state and to 1.1850 (|e|) in the T_1 state.

The total net charges on ligands for these states are also given in Table 2. From Table 2, we can also see that the positive net charge populations on ligands for the excited state are correspondingly reduced due to the electron transfer from Ru atom to the ligands. For the S_1 state, the calculated positive net charges on the main ligand (as a whole) and the two co-ligands (as a whole) are reduced by 0.0458 and 0.1505 (|e|), respectively, and the same trend happens in T_1 state, in which the positive charge on the ligand is reduced by 0.0704 (|e|) for the main ligand and 0.1337 (|e|) for the two coligands, respectively.

3.3. Some Frontier Molecular Orbitals for the Ground State (S_0) of the Complex. The frontier molecular orbitals of the ground state (S_0), for example, the highest-occupied molecular orbital (HOMO) and the occupied MOs near to HOMO (HOMO−x) as well as the lowest-unoccupied MO (LUMO) and the unoccupied MOs near to LUMO (LUMO+x) are very important because they not only closely relate to spectral properties but also to reaction activity of a complex. Some frontier MO stereo-contour graphs of the $[Ru(Phen)_2(6\text{-OH-dppz})]^{2+}$ are shown in Figure 2, and for discussing the substituent (−OH) effect, some frontier MO stereocontour graphs of parent $[Ru(phen)_2(dppz)]^{2+}$ at the same theory level are also given in Figure 3. In addition, the energy levels of some frontier MOs of complexes $[Ru(phen)_2(6\text{-OH-dppz})]^{2+}$ and $[Ru(phen)_2(dppz)]^{2+}$ are also shown in Figure 4.

Many theoretical studies have shown that the DNA base pairs are excellent electron donators, because the energies of their occupied frontier molecular orbitals (HOMO and HOMO−x) are quite high, and the components of such molecular orbitals are predominantly distributed on the base pairs, whereas almost all complexes as intercalators are excellent electron acceptors, because the energies of their unoccupied frontier molecular orbitals (LUMO and LUMO+x) are usually negative and quite low, even much lower than some of the frontier occupied MOs (HOMO and HOMO−x) of the DNA base pairs.[31,53] For example, Kurita and Kobayashi[31] reported the DFT results for stacked DNA base pairs with backbones, in which the energies of the HOMO and HOMO−x ($x = 1-6$) were quite high (−1.27 to −2.08 eV) and the components of HOMO and HOMO−x were mainly distributed on the base pairs. For our studied $[Ru(phen)_2(6\text{-OH-dppz})]^{2+}$, the LUMO and LUMO+$x$ ($x = 0-3$) energies calculated by the DFT method were quite low (−7.42 to −7.23 eV) and their components were distributed on the ligands, especially on the intercalative ligand. Such facts indicate that $[Ru(phen)_2(6\text{-OH-dppz})]^{2+}$ as an intercalator in ground state is an excellent electron acceptor and thus it can well interact with DNA base pairs, in agreement with its large DNA-bonding constant of $4.68 \times 10^5\ M^{-1}$.[7]

From Figures 2, 3, and 4, we can further see the following: (i) Some frontier occupied MOs of which the components mainly come from d orbitals of the Ru atom for $[Ru(phen)_2(6\text{-OH-dppz})]^{2+}$ are HOMO-1, HOMO-2, and HOMO-3, whereas those for the parent complex $[Ru(phen)_2(dppz)]^{2+}$ are HOMO, HOMO-2, and HOMO-3. Moreover, the HOMO of $[Ru(phen)_2$-

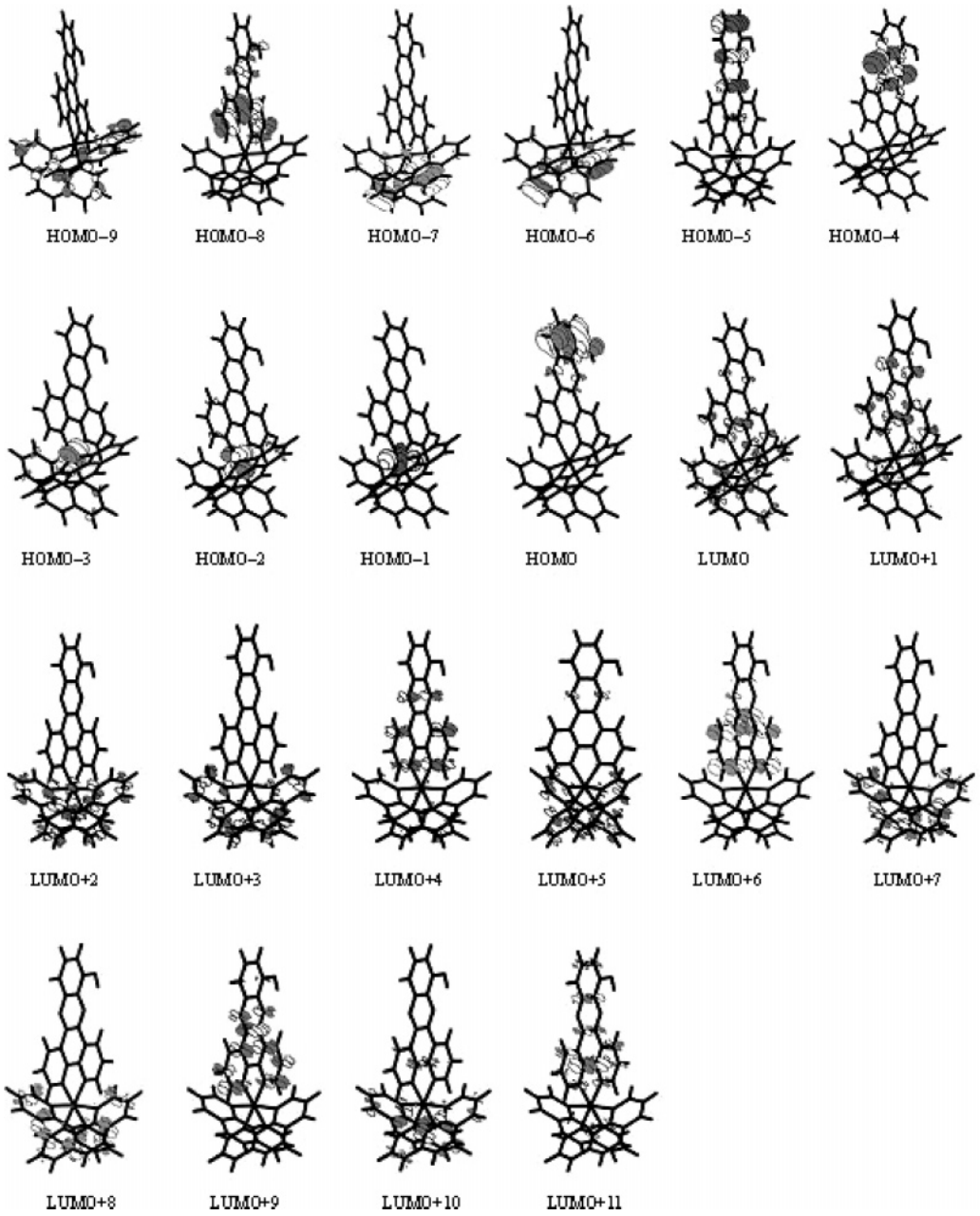

Figure 2. Some frontier MO contour plots of the ground state S_0 of $[Ru(phen)_2(6\text{-OH-dppz})]^{2+}$ in vacuo at the level of B3LYP/LanL2DZ.

$(6\text{-OH-dppz})]^{2+}$ comes mainly from π_{dppz} and n(O) orbitals. (ii) Some frontier unoccupied MOs of which the components mainly come from π_{dppz} for $[Ru(phen)_2(6\text{-OH-dppz})]^{2+}$ are the LUMO and LUMO+1, LUMO+4 and LUMO+6, whereas those for $[Ru(phen)_2(dppz)]^{2+}$ are LUMO+1, LUMO+5 and LUMO+6. It suggests that the substituent OH on dppz makes the LUMO have much more π^* components on the main ligand OH-dppz, compared with the LUMO of $[Ru(phen)_2(dppz)]^{2+}$. (iii) The substituent OH makes the energy gap between the HOMO and LUMO of $[Ru(phen)_2(6\text{-OH-dppz})]^{2+}$ obviously smaller than that of $[Ru(phen)_2(dppz)]^{2+}$ (seen in Figure 4).

Above-mentioned electronic structural characteristics of $[Ru(phen)_2(6\text{-OH-dppz})]^{2+}$ can be used to explain the spectral and DNA-photocleavage properties of the complex along with the TDDFT results.

3.4. Theoretical Explanation on the Spectral Properties. The experimental absorption spectra of the complex $[Ru(phen)_2(6\text{-OH-dppz})]^{2+}$ in aqueous solution show that there are three bands with comparable intensity, lying in the range of 250−550 nm.[7] The first one is a strong and broad absorption band centered at 440 nm (2.82 eV), which is generally assigned to a singlet metal-to-ligand charge transfer (^{1}MLCT) and very widely applied in bioinorganic chemistry. There are two strong and narrow bands centered at 325 nm (3.81 eV) and 262 nm (4.73 eV), respectively. These three bands can be theoretically well calculated, simulated, and explained. The calculated excitation energies (ΔE/eV) within the range 250−550 nm, oscillator strengths ($f \geq 0.05$) and main orbital transition contributions ($\geq$15%) of the complex in vacuo and in aqueous solution with the TDDFT at the level of B3LYP/LanL2DZ, as well as the experimental values are given in Tables 3 and 4, respectively. Moreover, the simulated electronic spectra of the complex in vacuo and in aqueous solution are also shown along with the experimental absorption spectra in Figure 5.

From Tables 3, 4 and Figure 4, we can see that the results of the spectral calculations and simulations for this complex in vacuo and in aqueous solution are very near except for some oscillator strengths and some details of transitions.

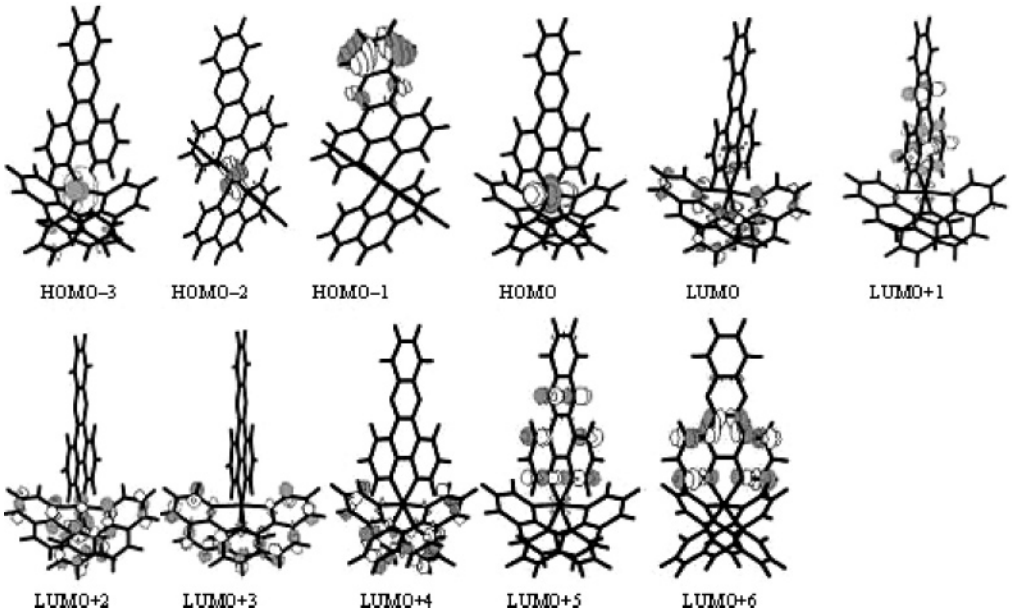

Figure 3. Some frontier MO contour plots of the ground state of $[Ru(phen)_2(dppz)]^{2+}$ in vacuo at the level of B3LYP/LanL2DZ.

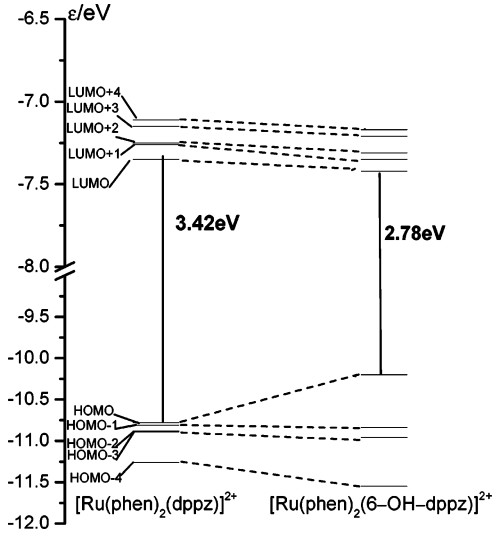

Figure 4. Energy levels of some frontier molecular orbitals of $[Ru(phen)_2(dppz)]^{2+}$ and $[Ru(phen)_2(6\text{-OH-dppz})]^{2+}$ in vacuo.

First, for the calculated spectra in aqueous solution, there are seven excited states lying in the range of 350−550 nm, including two pairs of quasi energy degenerate MLCT transitions, in which one pair at 429 and 427 nm with close oscillator strength (f = 0.095 and 0.100) can mainly be characterized by the transition of $d_{Ru}\rightarrow\pi^*_{co}+\pi^*_m$ and $d_{Ru}\rightarrow\pi^*_m+\pi^*_{co}$, another pair at 402 nm and 401 nm with close oscillator strength (f = 0.129 and 0.104) can mainly be characterized by the transition of $d_{Ru}\rightarrow\pi^*_{co}+\pi^*_m$ (>80%). In addition, there are three relatively weak bands at 476 (f = 0.077), 412 (f = 0.060), and 409 nm (f = 0.055) with the transition from d orbital to ligands. Therefore, the experimental broadband at ∼440 nm can be assigned to the superposition of the two pairs of stronger bands and the three separate weak bands with the character of MLCT transition. Similarly, for the spectral calculation results in vacuo, this experimental broadband can be assigned to the superposition of the four bands at 432 (f = 0.059), 428 (f = 0.244), 402 (f = 0.088), and 375 nm (f = 0.054) with MLCT character.

Next, for the calculated spectra in aqueous solution, there is one strong and relatively narrow band in the range of 300−350 nm. The calculated transition band at 314 nm mainly involves the inner transition of main ligand $\pi_m\rightarrow\pi^*_m$ (78%) with very large oscillator strength (f = 0.973), and thus it can be characterized by the LL transition and corresponds to the experimental band at ∼325 nm. Similarly, for the spectral calculation results in vacuo, this experimental band can be assigned to the superposition of the three bands at 335 (f = 0.080), 325 (f = 0.093), and 316 nm (f = 0.295) with LL character.

Finally, for the calculated spectra in aqueous solution, there are two pairs of quasidegenerate transitions, in which one pair lies at 267 (f = 0.096) and 266 nm (f = 0.130) and another pair lies at 264 (f = 0.053) and 262 nm (f = 0.087). The former pair is composed of the transitions at 267 nm mainly coming from $\pi_m\rightarrow\pi^*_{co}$ (80%) and the transitions at 266 nm mainly involving $d_{Ru}\rightarrow\pi^*_m$(50%), $\pi_m\rightarrow\pi^*_m+\pi^*_{co}$(22%), and $\pi_{co}\rightarrow\pi^*_m+\pi^*_{co}$ (18%). The latter pair is composed of the transitions at 264 nm mainly coming from $\pi_{co}\rightarrow\pi^*_m+\pi^*_{co}$ (59%) and the transitions at 262 nm coming from $\pi_{co}\rightarrow\pi^*_{co}$ (30%), $\pi_{co}\rightarrow\pi^*_m$ (20%), and $\pi_m\rightarrow\pi^*_{co}$ (25%). Therefore, the experimental band at 262 nm can be assigned to the superposition of the two pairs of transitions with LLCT character mixed with some MLCT. However, in the spectral calculation in vacuo, this experimental band can be assigned to the superposition of the seven bands at 275 (f = 0.176), 273 (f = 0.093), 273 (f = 0.107), 271 (f = 0.054), 266 (f = 0.141), 263 (f = 0.105), and 261 nm (f = 0.125) with very close energies and pure LL character except for the band at 271 nm mixed with some MM character.

The absorption spectra in aqueous solution of parent complex $[Ru(phen)_2(dppz)]^{2+}$ simulated with the similar method by Fantacci et al.[21] show that there are two pairs of strong excitation states with large oscillator strength $f \approx 0.1$ responsible for well-known ^{1}MLCT. One pair at ∼414 nm comes mainly from $d_{Ru}\rightarrow\pi^*_{phen}$ and $d_{Ru}\rightarrow\pi^*_{phen}+\pi^*_{dppz}$, another pair at ∼380 nm mixed with LL character comes from $d_{Ru}\rightarrow\pi^*_{dppz}$, $\pi_{dppz}\rightarrow\pi^*_{dppz}$, and $d_{Ru}\rightarrow\pi^*_{phen}$. For complex $[Ru(phen)_2(6\text{-OH-dppz})]^{2+}$, our computational results in aqueous solution also show two pairs of comparable MLCT excitation states with large oscillator strength $f \approx 0.1$. One pair at ∼429 nm comes mainly from the transitions $d_{Ru}\rightarrow\pi^*_{co}+\pi^*_m$ and $d_{Ru}\rightarrow\pi^*_m+\pi^*_{co}$, another pair at ∼402 nm comes mainly from the transition of $d_{Ru}\rightarrow\pi^*_{co}+\pi^*_m$. It is in agreement with the increasing main ligand components on LUMO due to introducing substituent OH, and it shows that

TABLE 3: Calculated Excitation Energies (ΔE/eV), Oscillator Strengths ($f \geq 0.05$), and Main Orbital Transition Contributions (≥15%) of $[Ru(phen)_2(6\text{-OH-dppz})]^{2+}$ with the TDDFT at the Level of RB3LYP/LanL2DZ in Vacuo as well as the Experimental Values

	major contribution[a]	ΔE, eV	f	λ_{cal} (nm)	λ_{exp}[b] (nm)	character
1	H^c-3(d_{Ru}) →L+1($\pi^*_m+\pi^*_{co}$)$_{(32\%)}$, H-2(d_{Ru}) → L^d+2($^*\pi^*_{co}$)$_{(28\%)}$	2.87	0.059	432	440 (2.82 eV)	MLCT
	H-2(d_{Ru})→L+1($\pi^*_m+\pi^*_{co}$)$_{(25\%)}$,H-1(d_{Ru})→ L+3(π^*_{co})$_{(22\%)}$,H-2(d_{Ru}) → LUMO($\pi^*_m+\pi^*_{co}$)$_{(18\%)}$	2.90	0.244	428		MLCT
	H-2(d_{Ru}) → L+3(π^*_{co}) $_{(38\%)}$, H-1(d_{Ru}) →L+5(π^*_{co}) $_{(37\%)}$	3.09	0.088	402		MLCT
	H-1(d_{Ru}) → L+6(π^*_m) $_{(81\%)}$	3.24	0.051	383		MLCT
2	H-5(π_m) → LUMO($\pi^*_m+\pi^*_{co}$)$_{(78\%)}$	3.70	0.080	335	325 (3.81 eV)	LL
	H-5(π_m) → L+1($\pi^*_m+\pi^*_{co}$)$_{(80\%)}$, H-5(π_m) → LUMO($\pi^*_m+\pi^*_{co}$)$_{(16\%)}$	3.82	0.093	325		LL
	H-5(π_m) → L+4(π^*_m)$_{(65\%)}$	3.92	0.295	316		LL
3	HOMO{π_m+n(O)} → L+11(π^*_m)$_{(35\%)}$,H-9(π_{co}) → LUMO ($\pi^*_m+\pi^*_{co}$)$_{(30\%)}$, HOMO{π_m+n(O)} → L+10(π^*_{co})$_{(15\%)}$	4.51	0.176	275	262 (4.73 eV)	LL
	H-8(π_m) → L+3 (π^*_{co})$_{(85\%)}$	4.53	0.093	273		LL
	H-8(π_m) → L+3(π^*_{co}) $_{(25\%)}$, H-9(π_{co}) → L+2(π^*_{co})$_{(16\%)}$	4.54	0.107	273		LL
	H-2(d_{Ru}) → L+13(d^*_{Ru})$_{(33\%)}$,H-3(d_{Ru}) → L+14(d^*_{Ru}*)$_{(26\%)}$,H-9(π_{co}) → L+1(π^*_m/ π^*_{co})$_{(15\%)}$,H-3(d_{Ru})→L+8(π^*_{co})$_{(15\%)}$	4.58	0.054	271		MM/LL
	H-7(π_{co}) → L+6(π^*_m)$_{(72\%)}$, H-6(π_{co}) → L+6 (π^*_m)$_{(15\%)}$	4.67	0.141	266		LL
	H-9(π_{co}) → L+4(π^*_m)$_{(37\%)}$, H-9(π_{co}) → L+5(π^*_{co})$_{(28\%)}$	4.71	0.105	263		LL
	H-8(π_m) → L+6(π^*_m)$_{(43\%)}$, H-7(π_{co}) → L+6 (π^*_m)$_{(17\%)}$	4.75	0.125	261		LL

[a] Contributions of main orbital transition contributions are shown in parentheses (≥15%), the subscript "m" in "π_m" means the dppz of main ligand, and the subscript "co" means co-ligands. H, HOMO; L, LUMO. [b] Experimental absorption spectra in aqueous solution.

TABLE 4: Calculated Excitation Energies (ΔE/eV), Oscillator Strengths ($f \geq 0.05$), and Main Orbital Transition Contributions (≥15%) of $[Ru(phen)_2(6\text{-OH-dppz})]^{2+}$ with the TDDFT at the Level of RB3LYP/LanL2DZ in Aqueous Solution as well as the Experimental Values

	major contribution[a]	ΔE, eV	f	λ_{cal} (nm)	λ_{exp}[b] (nm)	character
1	H-2(d_{Ru}) → LUMO(π^*_m)$_{(90\%)}$	2.60	0.077	476	440 (2.82 eV)	MLCT
	H-2(d_{Ru}) → L+3(π^*_{co})$_{(43\%)}$, H-1(d_{Ru}) → L+2($\pi^*_m+\pi^*_{co}$)$_{(40\%)}$	2.89	0.095	429		MLCT
	H-2(d_{Ru}) → L+2($\pi^*_m+\pi^*_{co}$)$_{(32\%)}$,H-2(d_{Ru}) → L+1($\pi^*_m+\pi^*_{co}$)$_{(26\%)}$,H-1(d_{Ru}) → L+3(π^*_{co})$_{(16\%)}$, HOMO(d_{Ru}) → L+4($\pi^*_{co}+\pi^*_m$)$_{(16\%)}$	2.90	0.100	427		MLCT
	HOMO(d_{Ru}) → L+6(π^*_{co})$_{(83\%)}$	3.00	0.060	412		MLCT
	HOMO(d_{Ru}) → L+5(π^*_m)$_{(84\%)}$	3.03	0.055	409		MLCT
	H-1(d_{Ru}) → L+4($\pi^*_{co}+\pi^*_m$)$_{(83\%)}$	3.08	0.129	402		MLCT
	H-2(d_{Ru}) → L+4($\pi^*_{co}+\pi^*_m$)$_{(84\%)}$	3.09	0.104	401		MLCT
2	H-6(π_m) → LUMO(π^*_m)$_{(78\%)}$	3.95	0.973	314	325 (3.81 eV)	LL
3	H-6(π_m) → L+6(π^*_{co})$_{(52\%)}$,H-10(π_m) → L+3(π^*_{co})$_{(28\%)}$	4.64	0.096	267	262 (4.73 eV)	LL
	H-2(d_{Ru}) → L+10(π^*_m)$_{(50\%)}$,H-10(π_m) → L+2($\pi^*_m+\pi^*_{co}$)$_{(22\%)}$,H-8(π_{co}) → L+4($\pi^*_{co}+\pi^*_m$)$_{(18\%)}$	4.65	0.130	266		MLCT/LL
	H-9(π_{co}) → L+4($\pi^*_{co}+\pi^*_m$)$_{(59\%)}$	4.69	0.053	264		LL
	H-9(π_{co}) → L+6(π^*_{co})$_{(30\%)}$,H-8(π_{co}) → L+5(π^*_m)$_{(20\%)}$,H-7(π_m) → L+6(π^*_{co})$_{(25\%)}$	4.72	0.087	262		LL

[a] Contributions of main orbital transition contributions are shown in parentheses (≥15%), the subscript "m" in "π_m" means the dppz of main ligand, and the subscript "co" means co-ligands. H, HOMO; L, LUMO. [b] Experimental absorption spectra in aqueous solution.

the substituent OH on dppz can make more "electron cloud" transfer from metal ion to main ligand.

It is very interesting to find the following: In general, the calculated and simulated spectra in aqueous solution should be better than those in vacuo; however, here the simulated spectra in vacuo are better than those in aqueous solution for the LL band at ~325 nm in both oscillator strength f and character. It may be attributed to the molecular intra-H-bond structure in $[Ru(phen)_2(6\text{-OH-dppz})]^{2+}$ since the molecular intra-H-bond coming from $N_5-C_9-C_6-O_{10}-H_{11}$ (see Figure 1) leads the hydrophobicity of the complex to enhance. The detailed interpretation regarding this phenomenon will be performed in further studies.

3.5. Theoretical Explanation on DNA Photocleavage by the Complex. The mechanism on DNA photocleavage by the Ru(II) complex is currently a very interesting and frontier subject. Many experimental studies[11,14,15,17,54,55] have demonstrated that UV or visual light irradiation can bring an electron transfer from a photoinduced Ru(II) complex to other various molecule or bring an electron transfer of intramolecule, resulting in a higher oxidation state (e.g., Ru(III)). Since the Ru(III) ion has a very strong oxidizing ability,[55] it can oxidize base pairs within the DNA duplex and thus result in the DNA cleavage. Barton et al. reported that the photoinduced complex $[Ru(phen)_2(dppz)]^{2+}$ can generate Ru(III) by intermolecular electron transfer[17] and result in the damage of DNA. Recently, Ji et al.[7] reported that the complex ($[Ru(phen)_2(6\text{-OH-dppz})]^{2+}$) can well cleave the single strand of DNA in experiment, but the mechanism of DNA photocleavage was not offered. So far, although a photoinduced oxidation reduction mechanism of DNA photocleavage by the Ru(II) complexes has been experimentally presented, the corresponding theoretical report has not been found. Here, based on the studies of $[Ru(phen)_2(6\text{-OH-dppz})]^{2+}$, we provide a theoretical insight for such a mechanism.

First, under UV or visual light irradiation, $[Ru(phen)_2(6\text{-OH-dppz})]^{2+}$ complex changes from the ground state (S_0) to the lowest excited state (S_1 and T_1). From the natural charge populations (see Table 2), we can see the following: the positive

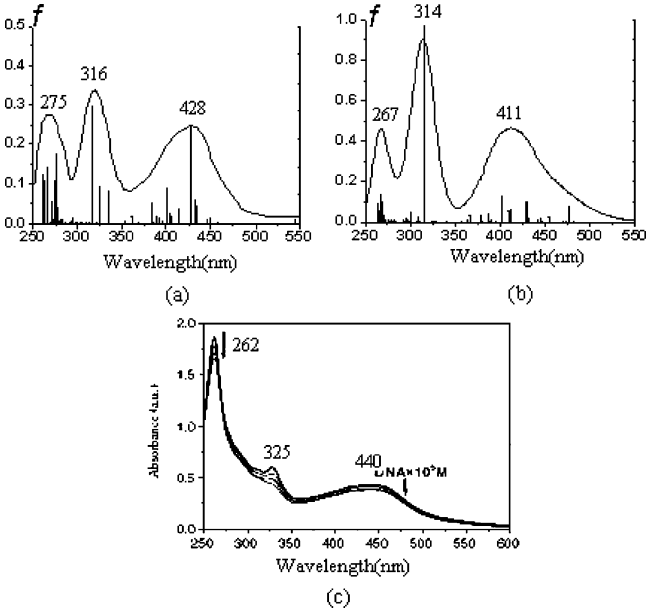

Figure 5. Simulated electronic spectra (a) in vacuo, (b) in aqueous solution calculated with TDDFT method at the level of B3LYP/LANL2DZ, and experimental absorption spectra (c) from ref 7.

charges of Ru atom increases from 0.9809 (|e|) in S_0 to 1.1772 (|e|) in S_1 (or 1.180 |e| in T_1), moreover, the positive charges on the main ligand of the complex in S_1 and T_1 are concomitantly changed, and they considerably reduce from 0.3397 (|e|) in S_0 to 0.2939 (|e|) in S_1 and 0.2693 (|e|) in T_1. Such changes show that the complex undergoes an obvious electron transfer between the central atom and ligands from S_0 to S_1 (or T_1) under light irradiation, as a result, the oxidizing ability of the Ru atom in the complex is greatly increased.

Second, from the spectral analyses in section 3.4, we can see that the electron transfers both in vacuo and in aqueous solution (in Table 4) mainly occur between the occupied orbitals (HOMO or HOMO-x) characterized by d_{Ru} and the unoccupied orbitals (LUMO or LUMO+x) characterized by π_m or π_{phen}. It is the reason why the change in natural charge populations is so large from the ground state to the excited states. Such facts also mean that the ability of the frontier unoccupied MO in excited states to accept electron will be greatly decreased, and thus the interaction between the main ligand and the DNA base pairs will be reduced in the excited states, because DNA base pairs are electron donors and the intercalative ligand is an electron acceptor.[53]

Third, as soon as the excited-state of the complex is formed under light irradiation, the distortion of geometry of the complex will happen in the lifetime of the excited states within only several hundred nanoseconds for T_1 and much shorter lifetime for the S_1. The bond lengths $(Ru-N)_m$ and $(Ru-N)_{co}$ of the complex in the excited states are considerably increased (seen in Table 1) relative to those in the ground state. Moreover, the coordination bond angle $(N-Ru-N)_m$ is considerably decreased. The changes in only several hundred nanoseconds maybe produce a strong impulsive force instantaneously along the intercalative direction of the complex to DNA. Meanwhile, the marked increase of bond length Ru−N in the excited state means that the coordination bond (or interaction) between the Ru ion and the N atoms of the ligands becomes weak. So such a change must be advantageous to making Ru ion free from coordination bond trammel and thus forms the Ru ion center with a high positive charge (expressed as Ru(III)).

In addition, from Figure 2−4, we can see that $\Delta\epsilon_{L-H}$ of $[Ru(phen)_2(6\text{-OH-dppz})]^{2+}$ (**1**) is smaller than that of $[Ru(phen)_2(dppz)]^{2+}$ (**2**) and the populations of LUMO on main ligand for **1** is greater than those for **2**. It means that the electrons (or "electron cloud") of **1** with substituent OH on the main ligand (dppz) easily transfer from HOMO to LUMO which plays an important role in DNA binding under light irradiation. It may be reasonable to speculate on that the DNA photocleavage ability of **1** is stronger than that of parent complex **2**, and such a speculation is expecting the experimental confirmation.

In summary, regarding the experimental photoinduced oxidation reduction mechanism of DNA photocleavage by $[Ru(phen)_2(6\text{-OH-dppz})]^{2+}$, we can theoretically propose the following: During light irradiation, the positive charge of the Ru atom in the complex is greatly increased due to the charge transfer from the central Ru atom to ligands (MLCT); the interaction between main ligand and DNA is also considerably weakened because the LUMO (or LUMO+x) of the complex characterized by π_m has accepted some electrons (or "electron-cloud") from the Ru atom; moreover, the interaction between Ru atom and the ligands is considerably reduced due to the distortions of geometry of the complex (especially the increase in the coordination bond length Ru−N). As a result, the Ru(III) ion center with high oxidizing ability in complex forms and approaches to DNA base pairs to oxidize them.

4. Conclusions

Theoretical results show the following: (1) Under UV or visual light irradiation, an obvious charge transfer happens from Ru central atom to the ligands of the complex, and the positive charges of the central Ru atom in the excited states (S_1 and T_1) are greatly increased relative to those in the ground state (S_0), and thus its oxidation ability is greatly enhanced in the excited states. (2) The positive charges on the main ligand in the excited states are considerably reduced due to the transfer of some "electron cloud" from central atom Ru(II) to main ligand, and thus the interaction between intercalative ligand and DNA base pairs is considerably weakened. (3) The distortion of geometry of the complex in the excited states is advantageous to the complex producing a Ru ion with high positive value (expressed as Ru(III)). As a result, the Ru(III) center with high oxidizing ability in the complex easily approaches to DNA base pairs to oxidize them. So our studies offer a theoretical explanation for the experimental photoinduced oxidation reduction mechanism of DNA photocleavage by the complex. In addition, the three absorption spectral bands in vacuo and in aqueous solution have also theoretically been calculated, simulated and assigned, and they are in good agreement with the experimental results.

Acknowledgment. The financial supports of the National Natural Science Foundation of China, the Natural Science Foundation of Guangdong Province, and the Research Fund for the Doctoral Program of Higher Education of China are gratefully acknowledged.

References and Notes

(1) Maheswari, P. U.; Palaniandavar, M. *J. Inorg. Biochem.* **2004**, *98*, 219.

(2) Friedman, A. E.; Chambron, J. C.; Sauvage, J. P.; Turro, N. J.; Barton, J. K. *J. Am. Chem. Soc.* **1990**, *112*, 4960.

(3) Barton, J. K.; Danishefsky, A. T.; Goldeberg, J. M. *J. Am. Chem. Soc.* **1984**, *106*, 2172.

(4) Mei, H. Y.; Barton, J. K. *Proc. Natl. Acad. Sci. USA* **1988**, *85*, 1339.

(5) Guerzo, A. D.; Mesmaeker, A. K. D.; Demeunynck, M.; Lhomme, J. *J. Chem. Soc. Dalton Trans.* **2000**, 1173.

(6) Arounaguiri, S.; Maiya, B. G. *Inorg. Chem.* **1999**, *38*, 842.
(7) Liu, X. W.; Li, J.; Li, H.; Zheng, K. C.; Chao, H.; Ji, L. N. *J. Inorg. Biochem.* **2005**, *99*, 2372.
(8) Zhang, Q. L.; Liu, J. G.; Liu, J. Z.; Li, H.; Yang, Y.; Xu, H.; Chao, H.; Ji, L. N. *Inorg. Chim. Acta* **2002**, *339*, 34.
(9) Zhang, Q. L.; Liu, J. H.; Liu, J. Z.; Zhang, P. X.; Ren, X. Z.; Liu, Y.; Huang, Y.; Ji, L. N. *J. Inorg. Biochem.* **2004**, *98*, 1405.
(10) Angeles-Boza, A. M.; Bradley, P. M.; Fu, P. K. L., Wicke, S. E.; Bacsa, J.; Dunbar, K. R.; Turro, C. *Inorg. Chem.* **2004**, *43*, 8510.
(11) Armitage, B. *Chem. Rev.* **1998**, *98*, 1171.
(12) Hergueta-Bravo, A.; Jiménez-Hernández, M. E.; Montero, F.; Oliveros, E.; Orellana, G. *J. Phys. Chem. B* **2002**, *106*, 4010.
(13) Fleisher, M. B.; Waterman, K. C.; Turro, N. J.; Barton, J. K. *Inorg. Chem.* **1986**, *25*, 3349.
(14) Fu, P. K. L.; Bradley, P. M.; van Loyen, D.; Durr, H.; Bossmann, S. H.; Turro, C. *Inorg. Chem.* **2002**, *41*, 3808.
(15) Lecomte, J. P.; Mesmaeker, A. K. D.; Feeney, M. M.; Kelly, J. M. *Inorg. Chem.* **1995**, *34*, 6481.
(16) Jacquet, L.; Davies, R. J. H.; Mesmaeker, A. K. D.; Kelly, J. M. *J. Am. Chem. Soc.* **1997**, *119*, 11763.
(17) Stemp, E. D. A.; Arkin, M. R.; Barton, J. K. *J. Am. Chem. Soc.* **1997**, *119*, 2921.
(18) Schoch, T. K.; Hubbard, J. L.; Zoch, C. R.; Yi, G. B.; Sørlie, M. *Inorg. Chem.* **1996**, *35*, 4383.
(19) Arounaguiri, S.; Easwaramoorthy, D.; Ashokkumar, A.; Dattagupta, A.; Maiya, B. H. *Proc. Indian Acad. Sci.* **2000**, *112*, 1.
(20) Yang, L.; Ren. A. M; Feng, J. K.; Liu, X. J.; Ma, Y. G.; Zhang, M; Liu, X. D.; Shen, J. C; Zhang, H. X. *J. Phys. Chem. A* **2004**, *108*, 6797.
(21) Fantacci, S.; De Angelis, F.; Sgamellotti, A.; Re, N. *Chem. Phys. Lett.* **2004**, *396*, 43.
(22) Fantacci, S; De Angelis, F.; Sgamellotti, A.; Marrone, A.; Re, N. *J. Am. Chem. Soc.* **2005**, *127*, 14144.
(23) Batista, E. R.; Martin, R. L. *J. Phys. Chem. A.* **2005**, *109*, 3128.
(24) Guillemoles, J. F.; Barone, V.; Joubert, L.; Adamo, C. *J. Phys. Chem. A* **2002**, *106*, 11354.
(25) Stoyanov, S. R.; Villegas, J. M.; Rillema, D. P. *Inorg. Chem. Commun.* **2004**, *7*, 838.
(26) Hertwig, R. H.; Koch, W. *Chem. Phys. Lett.* **1997**, *268*, 345.
(27) Beck, A. D. *Phys. Rev. A* **1988**, *38*, 3098.
(28) Perdew, J. P. *Phys. Rev. B* **1986**, *33*, 8822.
(29) Lee, C.; Yang, W. T.; Parr, R. G. *Phys. Rev. B* **1988**, *37*, 785.
(30) Petersilka, M.; Gossmann, U. J.; Gross, E. K. U. *Phys. Rev. Lett.* **1996**, *76*, 1212.
(31) Kurita, N.; Kobayashi, K. *Comput. Chem.* **2000**, *24*, 351.
(32) Runge, E.; Gross, E. K. U. *Phys. Rev. Lett.* **1984**, *52*, 997.
(33) Xu, L. C.; Li, Z. Y.; He, T. J.; Liu, F. C.; Chen, D. M. *Chem. Phys. Lett.* **2004**, *305*, 165.
(34) Sundholm, D. *Chem. Phys. Lett.* **1999**, *302*, 480.
(35) Xie, Z. Z.; Fang, W. H. *THEOCHEM* **2005**, *717*, 179.
(36) Li, J.; Xu, L. C.; Chen, J. C.; Zheng, K. C.; Ji, L. N. *J. Phys. Chem. A* **2006**, *110*, 8174.
(37) Dreuw, A.; Head-Gordon, M. *J. Am. Chem. Soc.* **2004**, *126*, 4007.
(38) Dreuw, A.; Head-Gordon, M. *Chem. Rev.* **2005**, *105*, 4009.
(39) Yavin, E.; Stemp, E. D. A.; Weiner, L.; Sagi, I.; Arad-yellin, R.; Shanzer, A. *J. Inorg. Biochem.* **2004**, *98*, 1750.
(40) Brennaman, M. K.; Alstrum-Acevedo, J. H.; Fleming, C. N.; Jang, P; Meyer, T. J.; Papanikolas, J. M. *J. Am. Chem. Soc.* **2002**, *124*, 15094.
(41) Pourtois. G.; Beljonne, D.; Moucheron, C.; Schumm, S.; Mesmaeker, A. K. D.; Lazzaroni, R.; Brédas, J. L. *J. Am. Chem. Soc.* **2004**, *126*, 683.
(42) Moller, C.; Plesset, M. S. *Phys. Rev.* **1934**, *46*, 618.
(43) Head-Gordon, M.; Pople, J. A.; Frisch, M. J. *Chem. Phys. Lett.* **1988**, *153*, 503.
(44) Head-Gordon, M.; Head-Gordon, T. *Chem. Phys. Lett.* **1994**, *220*, 122.
(45) Foresman, J. B.; Head-Gordon, M.; Pople, J. A.; Frisch, M. J. *J. Phys. Chem.* **1992**, *96*, 135.
(46) Barone, V.; Cossi, M. *J. Phys. Chem. A* **1998**, *102*, 1955.
(47) Cossi, M.; Rega, N.; Scalmani, G.; Barone, V. *J. Comp. Chem.* **2003**, *24*, 669.
(48) Hay, P. J.; Wadt, W. R. *J. Chem. Phys.* **1985**, *82*, 270.
(49) Wadt, W. R.; Hay, P. J. *J. Chem. Phys.* **1985**, *82*, 284.
(50) Frisch, M. J.; Trucks, G. W.; Schlegel, H. B.; Scuseria, G. E.; Robb, M. A.; Cheeseman, J. R.; Montgomery, J. A.; Vreven, Jr., T.; Kudin, K. N.; Burant, J. C.; Millam, J. M.; Iyengar, S. S.; Tomasi, J.; Barone, V.; Mennucci, B.; Cossi, M.; Scalmani, G.; Rega, N.; Petersson, G. A.; Nakatsuji, H.; Hada, M.; Ehara, M.; Toyota, K.; Fukuda, R.; Hasegawa, J.; Ishida, M.; Nakajima, T.; Honda, Y.; Kitao, O.; Nakai, H.; Klene, M.; Li, X.; Knox, J. E.; Hratchian, H. P.; Cross, J. B.; Bakken, V.; Adamo, C.; Jaramillo, J.; Gomperts, R.; Stratmann, R. E.; Yazyev, O.; Austin, A. J.; Cammi, R.; Pomelli, C.; Ochterski, J. W.; Ayala, P. Y.; Morokuma, K.; Voth, G. A.; Salvador, P.; Dannenberg, J. J.; Zakrzewski, V. G.; Dapprich, S.; Daniels, A. D.; Strain, M. C.; Farkas, O.; Malick, D. K.; Rabuck, A. D.; Raghavachari, K.; Foresman, J. B.; Ortiz, J. V.; Cui, Q.; Baboul, A. G.; Clifford, S.; Cioslowski, J.; Stefanov, B. B.; Liu, G.; Liashenko, A.; Piskorz, P.; Komaromi, I.; Martin, R. L.; Fox, D. J.; Keith, T.; Al-Laham, M. A.; Peng, C. Y.; Nanayakkara, A.; Challacombe, M.; Gill, P. M. W.; Johnson, B.; Chen, W.; Wong, M. W.; Gonzalez, C.; and Pople, J. A. *Gaussian 03*, Revision D.01; Gaussian, Inc.: Wallingford CT, 2005.
(51) Schaftenaar, G.; Noordik, J. H. *J. Comput.-Aid. Mol. Des.* **2000**, *14*, 123.
(52) Liu, J. G.; Zhang, Q. L.; Shi, X. F.; Ji, L. N. *Inorg. Chem.* **2001**, *40*, 5045.
(53) Řeha, D.; Kabeláč, M.; Ryjáček, F.; Šponer, J.; Šponer, J. E.; Elstner, M. Suhai, S.; Hobza, P. *J. Am. Chem. Soc.* **2002**, *124*, 3366.
(54) Westerlund, F.; Pierard, F.; Eng, M. P.; Nordén, Bengt.; Lincoln, P. *J. Phys. Chem. B* **2005**, *109*, 17327.
(55) Yang, I. V.; Thorp, H. H. *Inorg. Chem.* **2001**, *40*, 1690.